THE AMERICAN SOCIETY OF MECHANICAL ENGINEERS
345 E. 47th St., New York, N.Y. 10017

94-GT-163

EXPERIMENTAL HEAT TRANSFER AND FRICTION IN CHANNELS ROUGHENED WITH ANGLED, V-SHAPED AND DISCRETE RIBS ON TWO OPPOSITE WALLS

M. E. Taslim and T. Li
Department of Mechanical Engineering
Northeastern University
Boston, Massachusetts

D. M. Kercher
GE Aircraft Engines
General Electric Corporation
Lynn, Massachusetts

ABSTRACT

Experimental investigations have shown that the enhancement in heat transfer coefficients for air flow in a channel roughened with angled ribs is on the average higher than that roughened with 90° ribs of the same geometry. Secondary flows generated by the angled ribs are believed to be responsible for these higher heat transfer coefficients. These secondary flows also create a spanwise variation in heat transfer coefficient on the roughened wall with high levels of heat transfer coefficient at one end of the rib and low levels at the other end. In an effort to basically double the area of high heat transfer coefficients, the angled rib is broken at the center to form a V-shape rib and tests are conducted to investigate the resulting heat transfer coefficients and friction factors. Three different square rib geometries, corresponding to blockage ratios of 0.083, 0.125 and 0.167, with a fixed pitch-to-height ratio of 10, mounted on two opposite walls of a square channel in a staggered configuration are tested in a stationary channel for 5000 < Re < 30000. Heat transfer coefficients, friction factors and thermal performances are compared with those of 90°, 45° and discrete angled ribs. The V-shape ribs are tested for both pointing upstream and downstream of the main flow. Test results show that:

a) 90° ribs represent the lowest thermal performance, based on the same pumping power, and is essentially the same for the 2:1 change in blockage ratio, b) low blockage ratio (e/D_h =0.083) V-shape ribs pointing downstream produced the highest heat transfer enhancement and friction factors. Amongst all other geometries with blockage ratios of 0.125 and 0.167, 45° ribs showed the highest heat transfer enhancements with friction factors less than those of V-shape ribs, c) thermal performance of 45° ribs and the lowest blockage discrete ribs are among the highest of the geometries tested in this investigation, and, d) discrete angled ribs, although inferior to 45° and V-shape ribs, produce much higher heat transfer coefficients and lower friction factors compared to 90° ribs.

NOMENCLATURE

a	channel height (Figure 1)
A	cross-sectional area without ribs
b	channel width (Figure 1)
AR	channel aspect ratio (b/a)
AR_r	rib aspect ratio (e/w)
D_h	hydraulic diameter based on the cross-sectional area without ribs ($4A/P$)
e	rib height
$\bar{f}$	Darcy friction factor $\dfrac{\Delta P\left(\frac{L}{D_h}\right)}{\frac{1}{2}\rho U_m^2}$
$\bar{f_s}$	Darcy friction factor in an all-smooth-wall channel
$\bar{h}_t$	average heat transfer coefficient between a pair of ribs
k	air thermal conductivity
L	length of the roughened portion of the test section
$\overline{Nu}$	average Nusselt number between a pair of ribs ($\bar{h}_t D_h/k$)
$\overline{Nu}_s$	fully-developed average Nusselt number in a smooth passage
P	channel perimeter without ribs
Re	Reynolds number ($U_m D_h/\mu$)
S	rib pitch (center-to-center)
T_f	film temperature ($0.5(T_s + T_m)$)
T_m	air mixed mean temperature
T_s	surface temperature
U_m	air mean velocity
w	rib width
X	distance between camera and test section entrance angle of attack
μ	air dynamic viscosity
ΔP	pressure differential across the roughened portion of the test section
ρ	air density

Presented at the International Gas Turbine and Aeroengine Congress and Exposition
The Hague, Netherlands — June 13–16, 1994
This paper has been accepted for publication in the Transactions of the ASME
Discussion of it will be accepted at ASME Headquarters until September 30, 1994

INTRODUCTION

Heat transfer coefficient in a channel flow can be increased by roughening the walls of the channel. One such method, used over the past thirty years in internal cooling passages, is to mount rib-shape roughnesses on the channel walls. These ribs, also called turbulators, enhance the level of heat transfer coefficients by re-starting the boundary layer after flow reattachment between ribs.

Geometric parameters such as channel aspect ratio (AR), rib height-to-passage hydraulic diameter or blockage ratio (e/D_h), rib angle of attack (α), the manner in which the ribs are positioned relative to one another (in-line, staggered, crisscross, etc.), rib pitch-to-height ratio (S/e) and rib shape (round versus sharp corners, fillets, rib aspect ratio (AR_r), and skewness towards the flow direction) have pronounced effects on both local and overall heat transfer coefficients. Some of these effects were studied by different investigators such as Abuaf et al. (1986), Burggraf (1970), Chandra et al. (1987, 1989), Han et al. (1978, 1984, 1985, 1992), Metzger et al. (1983, 1990), Taslim et al. (1988, 1991), Webb et al. (1971). Among those geometries close to the present investigation are the papers by Lau et al. (1990, 1992) and Han et al. (1991). These last two references deal with heat transfer characteristics of turbulent flow in a square channel with angled discrete ribs. Heat transfer performance of 30°, 45°, 60° and 90° discrete, parallel and crossed ribs were investigated. The second investigation studied the augmentation of heat transfer in square channels roughened with parallel, crossed and V-shaped ribs. While their rib pitch-to-height ratio of 10 was identical to that in this study, the rib height to channel hydraulic diameter was 0.0625 in both investigations which is below the range tested in the present investigation (0.083 - 0.167). However, results of the smallest rib tested in this investigation are compared with those tested in the two above-mentioned references.

TEST SECTIONS

Figure 1 shows schematically the layout and cross-sectional area of a typical test section while rib geometry details are shown in Figure 2. Table 1 contains the specifications of the thirteen staggered rib geometries tested in this investigation. A liquid crystal technique was employed to measure the heat transfer coefficients between pairs of ribs in these test sections (Moffat, 1990). In this technique, the most temperature-sensitive color displayed by the liquid crystals is chosen as the reference color corresponding to a known temperature. By sensitive variation of the Ohmic power to a constant heat flux thin foil heater beneath the liquid crystals, the reference color is moved from one location to another such that the entire area between two ribs is eventually covered with the reference color at constant flow conditions. This process results in a series of photographs each corresponding to a certain location of the reference color. The area covered by the reference color for each photograph is then measured and an area-weighted average heat transfer coefficient is calculated along with the iso-Nu contours. Details of this process is explained in the **Procedure** section. Among the advantages of liquid crystal thermography is the ability to depict the flow "footprints" and local values of heat transfer coefficient on the surface under investigation. This simultaneous "flow visualization" enhances the understanding of the underlying physics and helps the investigator in interpretation of the results. Furthermore, unexpected asymmetries in flow are revealed as well as the slightest heat and flow leaks, nonuniformities in surface heat flux, imperfections associated with the attachment of the heater to the test section surface and nonuniformities in wall material thermal conductivity.

Coolant air, supplied by a compressor to a 0.95 *m3* storage tank, was circulated through an air filter, to a water-to-air heat ex changer, and through a second air filter to remove any residual water vapor and oil. A pressure regulator downstream of the second filter was used to adjust the flow rate. The air then entered a critical

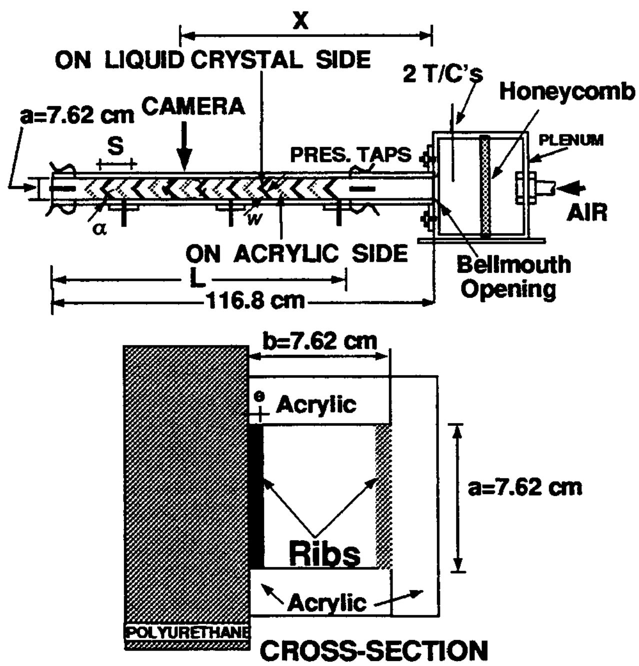

Figure 1 Schematic of a Typical Test Section

venturi-meter for mass flow measurement, to a plenum equipped with a honeycomb flow straightener, and then to the test section via a bellmouth opening.

All test sections, with a length of 116.8 *cm*, had a 7.62 *cm* × 7.62 *cm* square cross-sectional area. Three walls of these channels were made of 1.27 *cm* thick clear acrylic plastic. The fourth wall, on which the heaters and liquid crystal sheets were attached and all measurements were taken, was made of a 5 *cm* thick machineable polyurethane slab. This wall, for all cases tested, had a fixed width of 7.62 *cm*. Ribs were cut to length from commercially available acrylic plastic stock, in the form of square rods, and glued onto two opposite walls in a staggered arrangement.

The entrance region of all test sections was left smooth to produce well-established hydrodynamic and thermal boundary layers. Heat transfer measurements were performed for an area between a pair of ribs in the middle of the roughened zone corresponding to X/D_h = 9.5-11.6.

Four 7.62 *cm* × 27.94 *cm* custom-made etched-foil heaters with a

TESTS	e (mm)	e/D_h	α	X (cm)	X/D	Remarks	
1	6.35	0.0833	90° Stag.	77.16	10.125	Straight Ribs	□
2	9.525	0.125	90° Stag.	77.16	10.125	Straight Ribs	×
3	12.7	0.167	90° Stag.	72.39	9.5	Straight Ribs	+
4	6.35	0.0833	45° Stag.	88.11	11.56	Straight Ribs	○
5	9.525	0.125	45° Stag.	76.52	10	Straight Ribs	✳
6	12.7	0.167	45° Stag.	72.39	9.5	Straight Ribs	◁
7	6.35	0.0833	45° Stag.	88.11	11.56	V-shape pointing downstream	▽
8	6.35	0.0833	45° Stag.	88.11	11.56	V-shape pointing upstream	△
9	9.525	0.125	45° Stag.	86.68	11.375	V-shape pointing downstream	◇
10	12.7	0.167	45° Stag.	85.1	11.16	V-shape pointing downstream	▷
11	6.35	0.0833	45° Stag.	78.74	10.33	Discrete Ribs	▼
12	9.525	0.125	45° Stag.	81.92	10.75	Discrete Ribs	◆
13	12.7	0.167	45° Stag.	78.74	10.33	Discrete Ribs	▶

AR=1 AR_t =1 S/e=10 for all geometries symbols

Table 1 Specifications

thickness of 0.15 *mm* were placed on the polyurethane wall where measurements were taken using a special double-stick 0.05 *mm* thick tape with minimal temperature deformation characteristics. A detailed construction sketch of the heaters is shown in El-Husayni (1991). The heaters covered the entire test section length including the smooth entry length. However, they did not extend over the actual rib surface nor on the acrylic plastic sidewalls. Thus the reported heat transfer coefficients are the averages over the wall surface area between a pair of ribs. The heat transfer coefficient on the rib surfaces are reported by other investigators such as Metzger et al. (1988). As for having only one heated wall, it is noted that an experimental investigation by El-Husayni et al. (1992) on heat transfer in a rib-roughened channel with one, two and four heated walls showed that, in a stationary roughened channel, the heat transfer coefficient is not significantly sensitive to the number of heated walls. Encapsulated liquid crystals sandwiched between a mylar sheet and a black paint coat, collectively having a thickness of 0.127 *mm*, were then placed on the heaters. Static pressure taps, located ½-rib pitch upstream of the first rib and ½-rib pitch downstream of the last rib, measured the pressure drop across the rib-roughened test section. The reported friction factor is the overall passage average, $\bar{f}$ and not just the roughened surfaces.

The test sections were covered on all sides by 5 *cm* thick styrofoam sheets to minimize heat losses to the environment, except for a small window on tshe opposite wall at the location where photographs of the liquid crystals were taken. The radiational heat loss from the heated wall to the unheated walls as well as losses to ambient air were taken into consideration when heat transfer coefficients were calculated. A 35*mm* programmable SLR camera, in conjunction with proper filters and background lighting to simulate daylight conditions, were used to take photographs of isochrome patterns formed on the liquid crystal sheet. Surface heat flux in the test section was generated by the heaters through a custom-designed power supply unit. Each heater was individually controlled by a variable transformer.

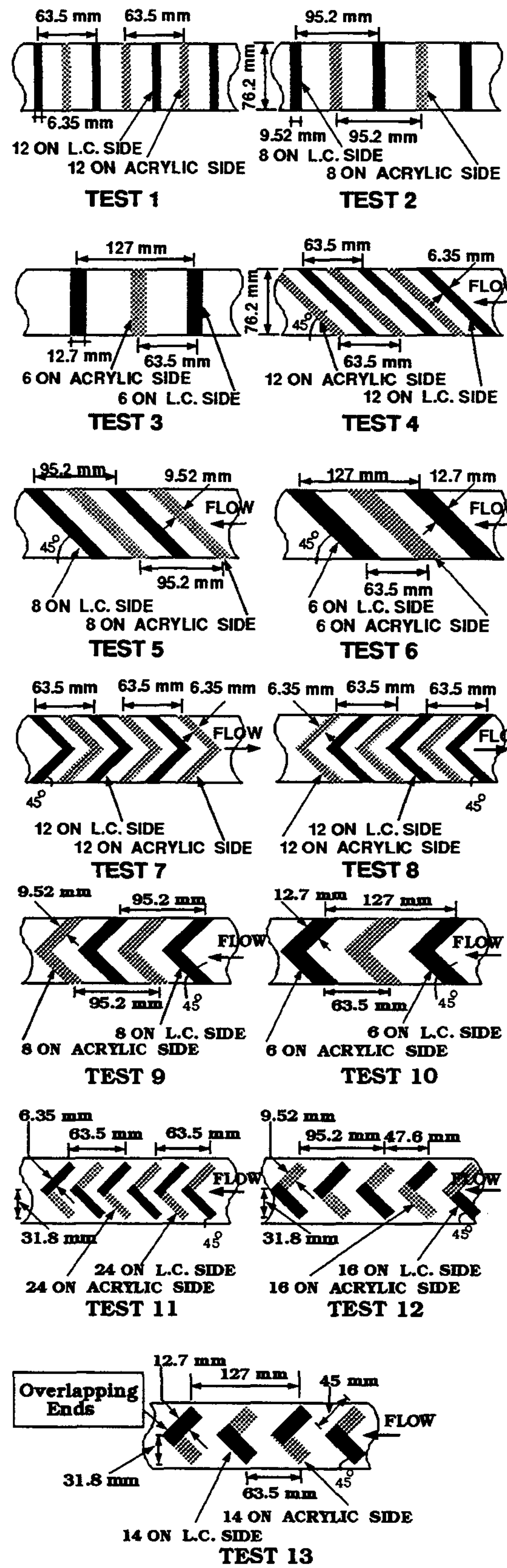

Figure 2 Rib Geometries

PROCEDURE

Before testing, the liquid crystal sheets were calibrated in a water bath to attain uniform isochromes on a small piece of the liquid crystal sheet used in this investigation. The temperature corresponding to each color was measured with a precision thermocouple and photographs were taken at laboratory conditions simultaneously to simulate closely the actual testing environment. A reference color along with its measured temperature of 36.9°C was chosen for the experiments. It should be noted that all possible shades of the selected reference color did not indicate a temperature variation more than 0.3°C. Therefore, the maximum uncertainty in wall temperature measurement was ±0.15°C.

A contact micromanometer with an accuracy of 0.025 *mm* of water column measured the pressure differential across the rib-roughened channel. A critical venturi-meter, with choked flow for all cases tested, measured the total mass flow rate entering the test section. With the known surface heat flux along the test section and application of the energy balance from the test section inlet to the camera location, the air mixed mean temperature was calculated taking into account the small heat losses through the test section walls to ambient air.

For a typical test Reynolds number, at a constant mass flow rate, the lowest heat flux was induced by adjusting the heater power until the first band of reference color was observed on the liquid crystal sheet in the area of interest. Each heater was adjusted individually to insure a uniform heat flux over the entire tested surface. At thermal equilibrium a photograph was taken and data recorded. Power to the heaters was then increased such that the reference color moved to a location next to the previous one (higher heat transfer coefficient) and another photograph was taken. This procedure was repeated until the entire surface between a pair of ribs was covered by the reference color. The process was then repeated for the range of test Reynolds numbers. Each photograph was then digitized in order to measure the area covered by the reference color. This was done by using a magnetic tablet and a commercial software package running on an IBM-PC/AT. Once the areas were measured, an area-weighted average heat transfer coefficient was calculated.

For verification of the liquid crystal technique accuracy, an all-smooth-wall channel has been tested with heaters on one wall. The heat transfer coefficient results (Taslim, 1990) were within ±5% of the Dittus-Boelter (1930) correlation. Previous results (Taslim et al., 1991c) of various geometry roughened channels using the same technique compared favorably with those of Metzger et al. (1990).

Experimental uncertainties, following the method of Kline and McClintock (1953), were estimated to be ±6% and ±8% for the heat transfer coefficient and friction factor respectively.

RESULTS AND DISCUSSION

Local average heat transfer coefficient results for an area between a pair of ribs corresponding to $X/D_h = 9.5\text{-}11.6$ for the thirteen rib geometries are compared with the all-smooth-wall channel Dittus-Boelter (1930) correlation

$$\overline{Nu_S} = 0.023 Re^{0.8} Pr^{0.4}$$

in Figures 3, 8, 10, 13 and 15. With this correlation, the enhancement in rib-roughened heat transfer coefficients can be readily evaluated as illustrated in Figure 12. The thermal performance, based on the same pumping power, is given by

$$\left(\overline{Nu}/\overline{Nu_S}\right)/\left(\overline{f}/\overline{f_S}\right)^{\frac{1}{3}}$$

(Han et al.,1985), where $\overline{f_s}$ is the all-smooth-wall friction factor from Moody (1944). Air properties for Nusselt and Reynolds number calculations are based on the local film temperature, T_f for all cases.

90° and 45° Ribs

Heat transfer and friction factor results of the 45° and 90° ribs are shown in Figures 3 and 4. As shown in Table 1 and Figure 2, under otherwise identical conditions, the three 90° rib geometries representing three different blockage ratios will serve as a baseline against which other configurations will be compared.

As expected for 90° ribs, larger blockage ratios produced higher heat transfer coefficients as well as higher pressure losses. Some representative iso-Nu contours (contours of constant Nusselt number) for tests 1, 2 and 3 (Figure 2) are shown in Figure 5. The apparent change of scale from one test to another is due to the change of camera position to cover the area between a pair of ribs as they become farther apart. The shaded area represents the staggered rib on the opposite wall. It can be seen that the local heat transfer coefficient, starting from a relatively low value in the rib wake region, reaches its maximum near the point of flow reattachment and then decreases again close to the downstream rib.

To investigate the effects 45° angled ribs have on the heat transfer

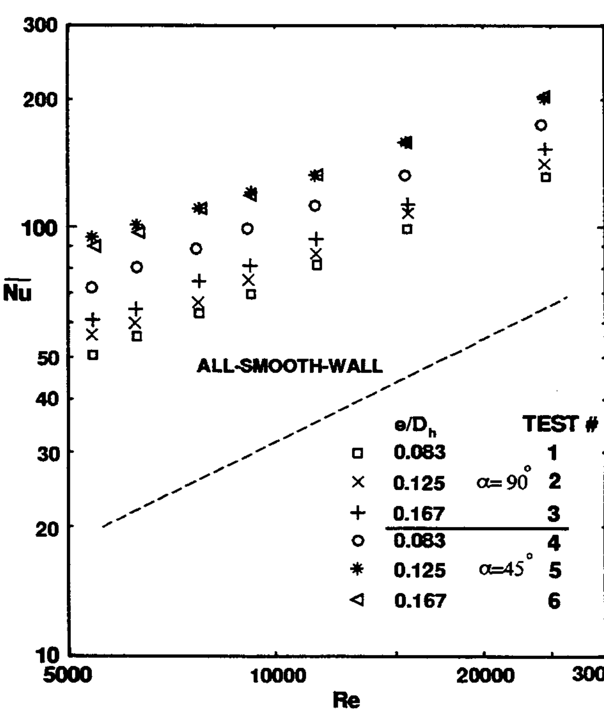

Figure 3 Comparison of Blockage ratio Effects on Surface Average Nusselt Number for 90° and 45° Rib geometries

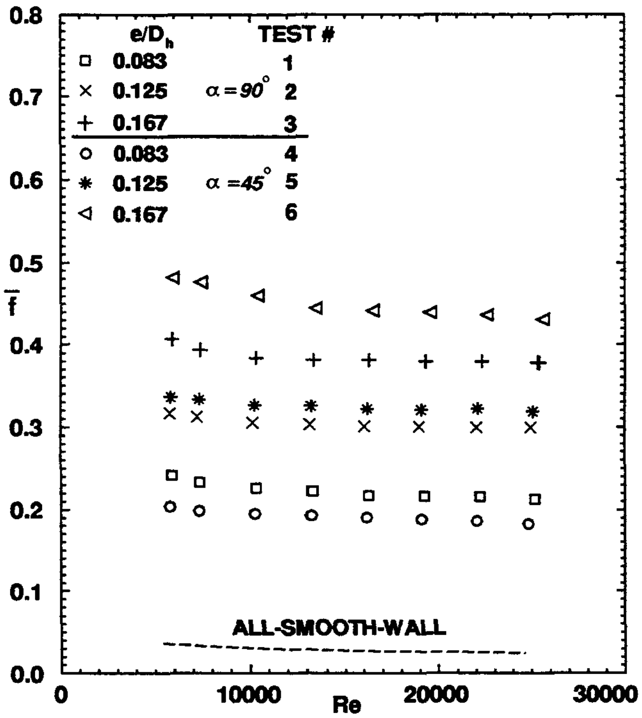

Figure 4 Comparison of Blockage ratio Effects on Channel Average Friction Factor for 90° and 45° Rib geometries

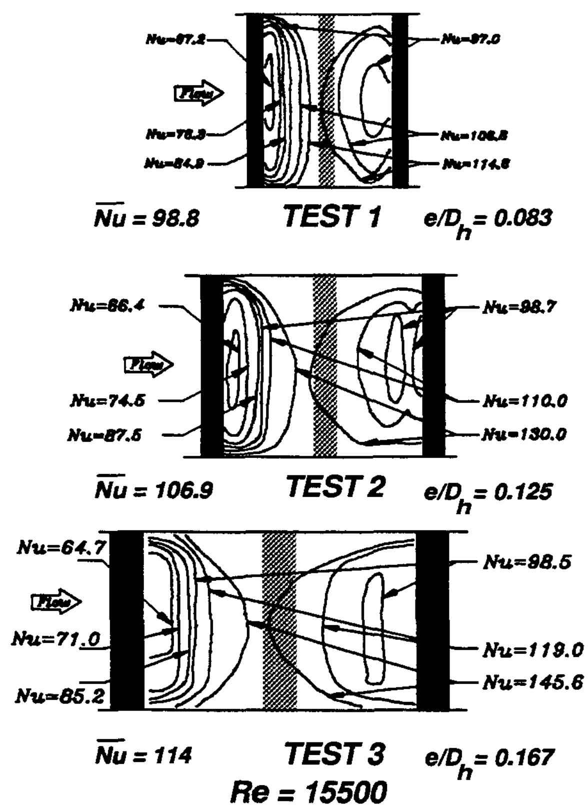

Figure 5 Representative Iso-Nu Contours for the 90° Ribs

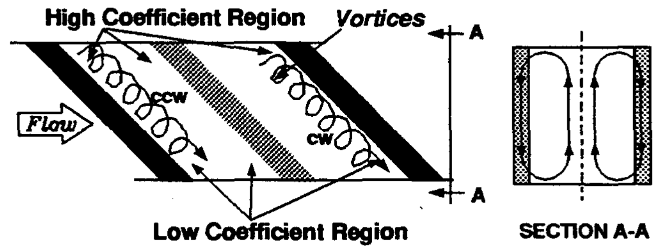

Figure 6a Cell Formation for 45° Ribs

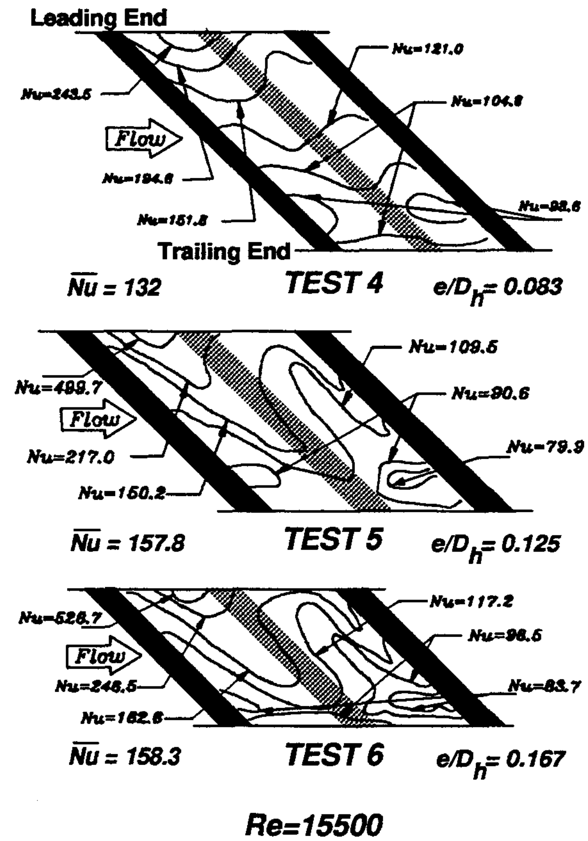

Figure 6b Representative Iso-Nu Contours for 45° Ribs

performance and pressure loss, test sections 4 - 6 (Figure 2) were tested which were identical to test sections 1 - 3 in all aspects except for the ribs angle of attack which was 45° to the flow direction. Spanwise, counter-rotating, double-cell secondary flows created by the angling of ribs as depicted in Figure 6a, appear to be responsible for the significant spanwise variation in heat transfer coefficient observed in Figure 6b. Formation of these rotating cells when ribs are angled is explained in detail by Metzger et al. (1990) and Fann et al. (1994). Whereas the two fluid vortices immediately upstream and downstream of a 90° rib are essentially stagnant (relative to the mainstream flow velocity) which raises the local fluid temperatures in the vortices and wall temperature near the rib resulting in low heat transfer coefficients, the vortices between 45° angled ribs are not stagnant but moving along the ribs and then join the main stream (Fann et al. 1994). These moving vortices between staggered parallel angled ribs set up a strong double-cell counter-rotating secondary flow which brings lower center-channel fluid temperatures near the angled ribs leading end regions, enhances the local heat transfer coefficients, and lowers the wall temperatures (Fann et al. 1994) at constant heat flux. Near the trailing end region of the ribs, the local fluid temperatures increase as the vortices secondary flow sweeps the floor between ribs shown in Figure 6a. This phenomenon appears to result in lower heat transfer coefficients in the rib leading end region as indicated by measured results shown in Figure 6b. As shown in Figure 3, the surface-averaged heat transfer coefficients for these geometries are higher than corresponding 90° ribs. In Figure 4, the angled ribs with the lowest blockage ratio (0.083) produced less form drag resulting in lower pressure losses compared to 90° ribs. The other two rib geometries produced slightly higher friction factors. The thermal performances for these two geometries, compared in Figure 18 (combined Figures 3 and 4), confirms the superiority of 45° angled ribs over the 90° ribs.

V-Shape Ribs

The possibility of further increasing the wall heat transfer with V-shape ribs is based on the observations made in Figure 6b. There exists a region downstream of the leading end of the angled rib where the heat transfer coefficient is maximum and a region downstream of the trailing end of the rib where the heat transfer coefficient is the lowest. To further enhance the average heat transfer coefficient, it was speculated that by breaking the 45° rib into two half ribs in a V- shape, one basically doubles the high heat transfer coefficient area. It was also speculated that with the apex facing downstream one would have higher overall heat transfer than facing upstream. This reasoning is based on the vortex characteristic change and the increase in the number of secondary flow cells formed by the V-shaped ribs relative to the 45° angled ribs. Whereas the 45° angled rib had a double-cell counter-rotating secondary flow, the V-shaped rib vortices upstream and downstream of the ribs will generate two double-cell counter-rotating secondary flow region when the rib apex is pointed downstream as shown in Figure 7a. Again these rotations pump cooler center-channel air toward the leading end regions of the V-shaped ribs and warmer air toward the center of the ribs as illustrated in Figure 7a. The increase in the number of cells to four and the corresponding changes in the secondary flow directions result in higher heat transfer coefficients near the leading ends and lower heat transfer coefficients near the center apex with a net increase in average heat transfer compared to the 45° angled ribs as later shown in Figure 12.

For the rib apex facing upstream, it is reasoned that the change in the V-shaped rib orientation again creates two double-cell counter-rotating vortices but in an opposite direction from the rib apex facing downstream as shown in Figure 7a. This results in warmer air being pumped into the ribs leading end regions and cooler air being pumped into the ribs center apex region. This should change the heat transfer coefficient distribution compared to the downstream pointed apex i.e., increase the apex region coefficients and lower the leading end regions coefficients.Therefore,

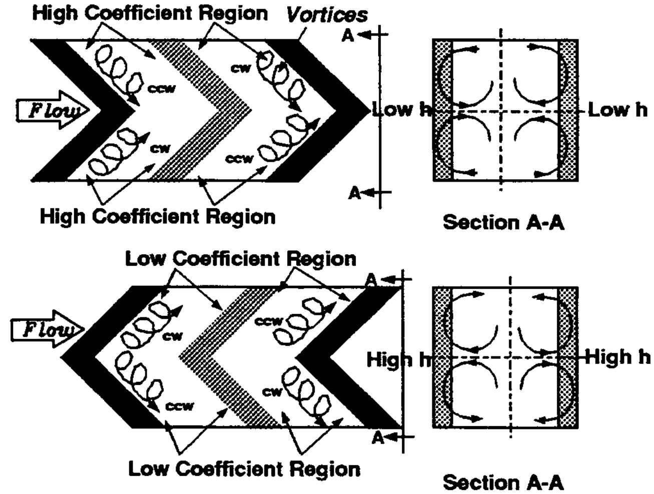

Figure 7a Cell Formation for V-Shape Ribs

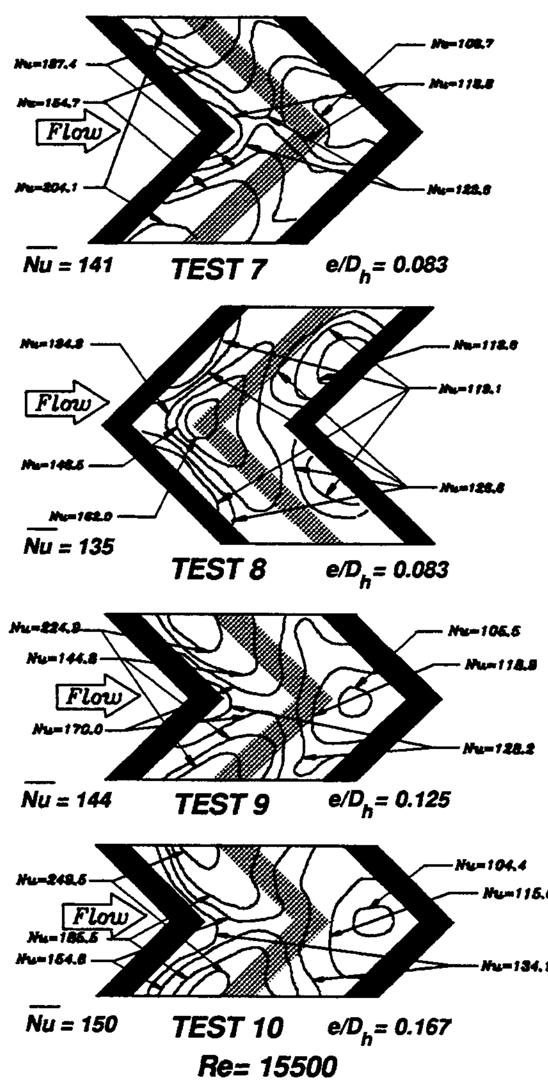

Figure 7b Representative Iso-Nu Contours for the V-Shape Ribs

test sections 7 and 8, shown in Figure 2, were tested.

The representative iso-Nu contours for these two low blockage ribs and two other higher blockage V-shape ribs (test sections 9 and 10, downstream apex) are shown in Figure 7b. As expected, two symmetric leading end regions of high heat transfer coefficients and a center region of lower coefficients are formed which contribute to a higher overall heat transfer coefficient for the V-shape ribs when compared with the 45° angled ribs shown in Figure 12. Comparing tests 7 and 8 in Figure 7b, iso-Nusselt-number contours further indicate that the distribution results compared well with the secondary flow speculation noted above i.e. a reverse Nusselt number distribution exists for the upstream-facing apex ribs (Test 8) compared to Test 7. Furthermore, as shown in Figures 8 and 9, the V-shape ribs pointing downstream produce slightly higher heat transfer coefficients as well as friction factors than the ribs pointed upstream. Higher friction factors for those ribs pointing downstream is in line with Colburn (1933) analogy between heat transfer coefficient and friction factor. From the thermal performance viewpoint, however, as shown in Figure 18 the 45° angled ribs are still superior to V-shape ribs.

Discrete Ribs

The next series of three test configurations deal with discrete angled ribs (test sections 11, 12 and 13 in Table 1and Figure 2) mounted on two opposite walls in a staggered array. Note that in Figure 2 , first, a gap between these ribs and the smooth walls and, second, the solid black ribs are mounted on the liquid crystal wall and the cross-hatched ribs are on the opposite acrylic wall with their overlapping leading edge on the channel centerline. For the two highest blockage ratios, these ribs performed inferior to the V-

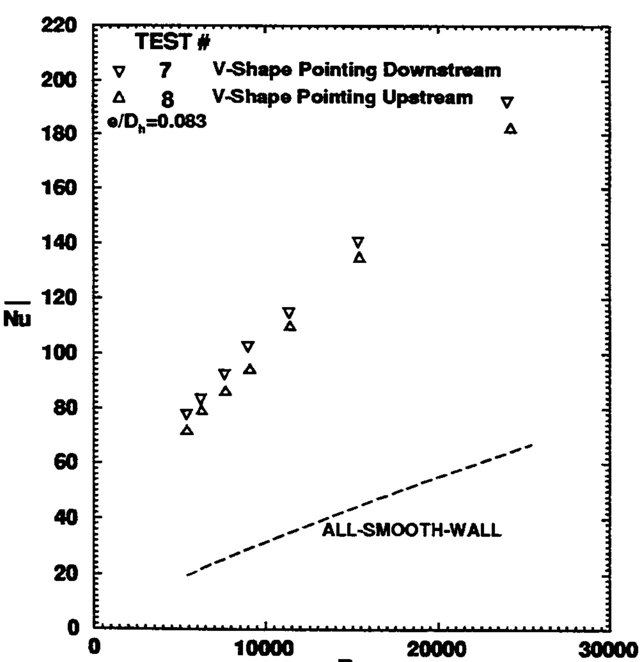

Figure 8 Comparison of Turbulator Orientation on Surface Average Nusselt Number for V-Shape Rib geometries

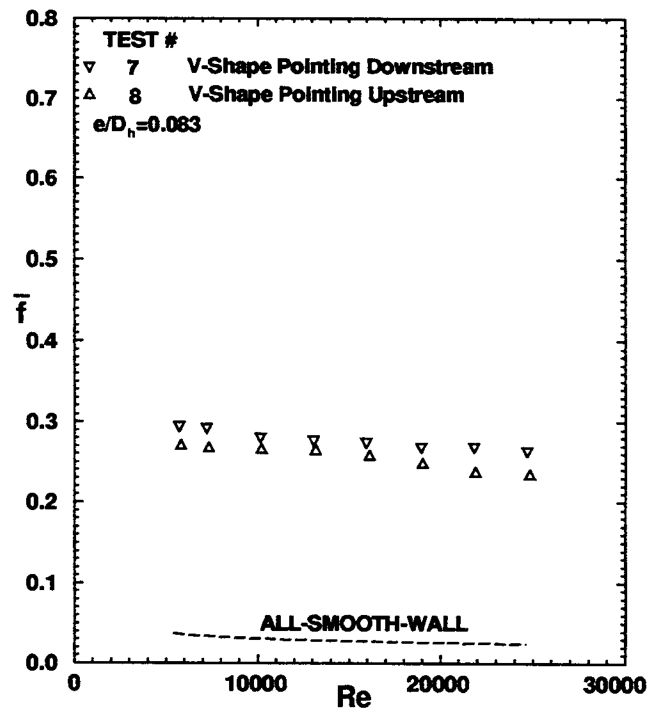

Figure 9 Comparison of Turbulator Orientation on Channel Average Friction Factor for V-Shape Rib geometries

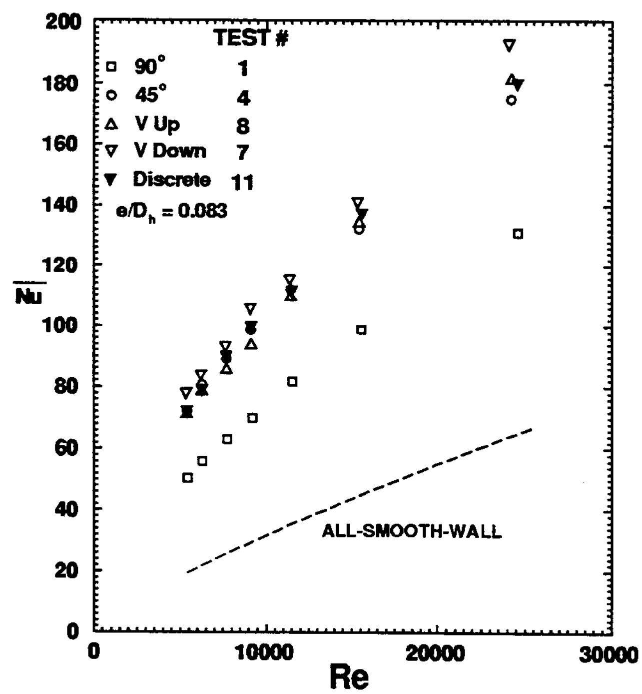

Figure 10 Comparison of Surface Average Nusselt Number for Five Rib geometries of 0.083 Blockage Ratio

shape ribs in average heat transfer as noted in Figures 10, 13 and 15. This observation appears to be due to the presence of relatively large gaps between consecutive ribs on each wall and also between

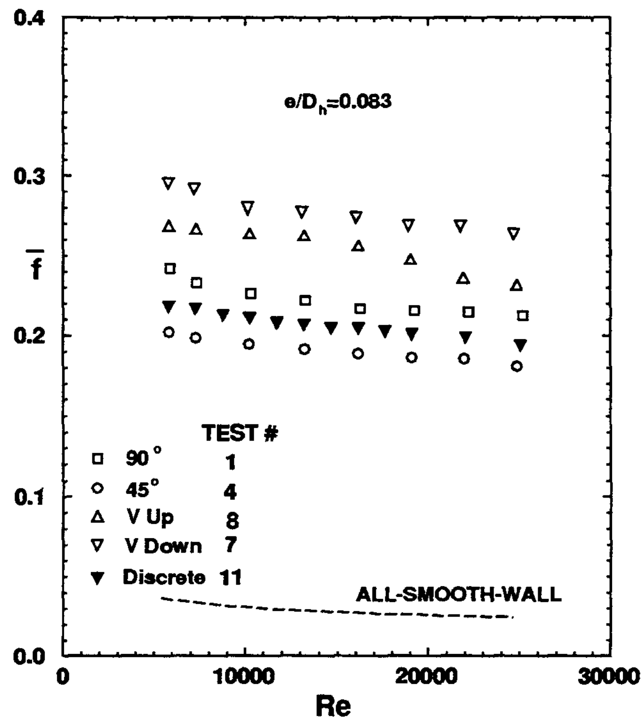

Figure 11 Comparison of Channel Average Friction Factor for Five Rib geometries of 0.083 Blockage Ratio

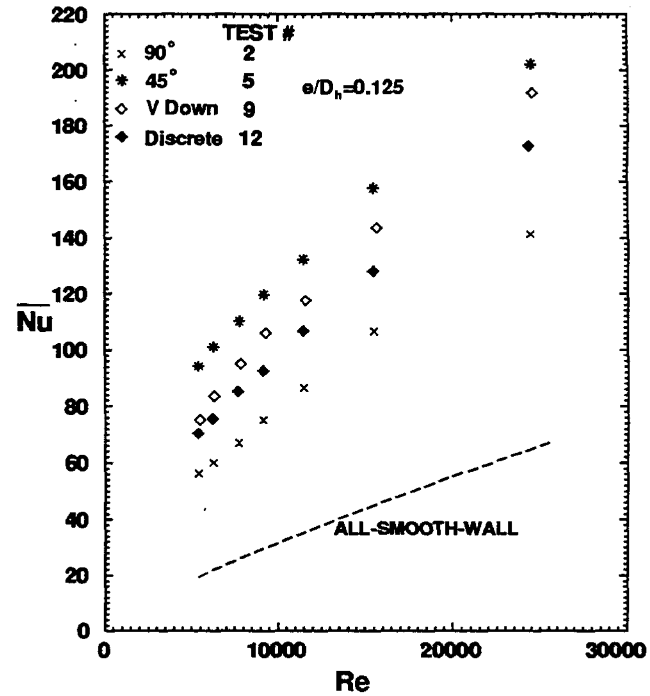

Figure 13 Comparison of Surface Average Nusselt Number for Four Rib geometries of 0.125 Blockage Ratio

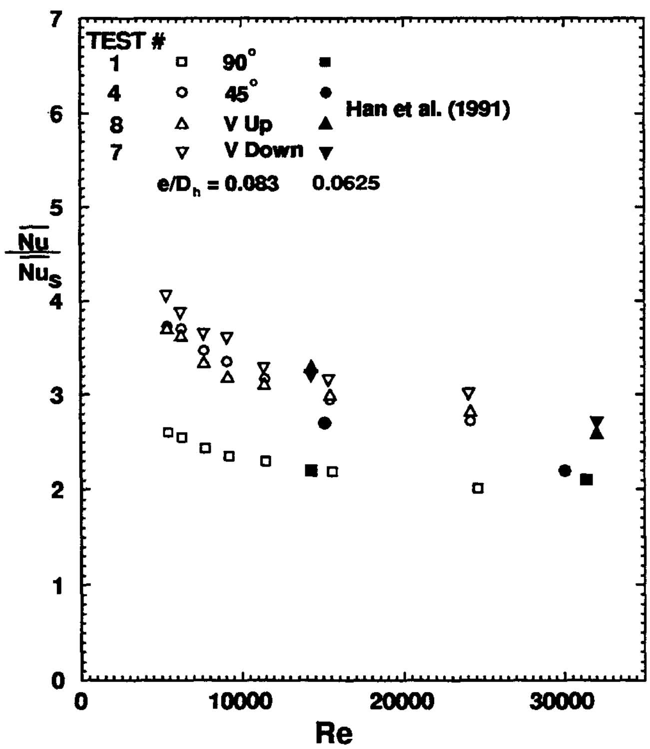

Figure 12 Comparison of Heat Transfer Enhancement for Four Rib geometries of 0.0625 and 0.083 Blockage Ratios

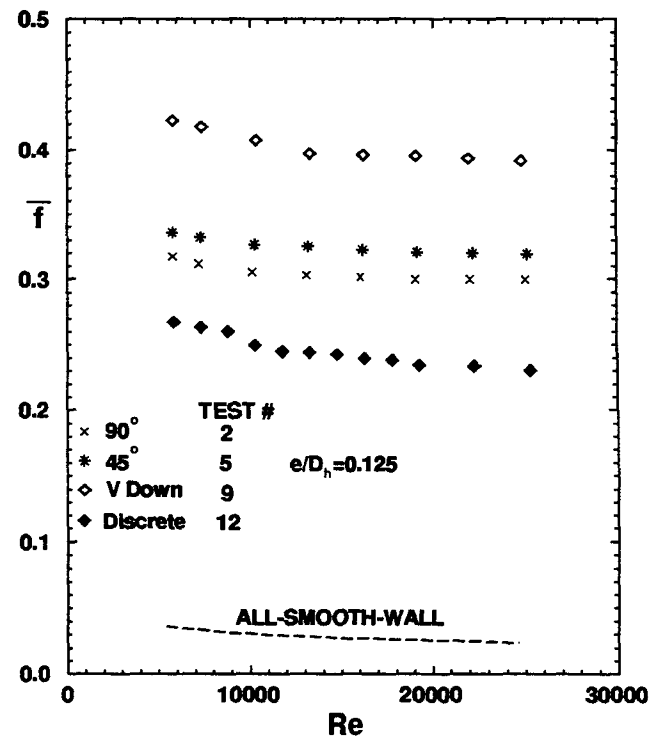

Figure 14 Comparison of Channel Average Friction Factor for Four Rib geometries of 0.125 Blockage Ratio

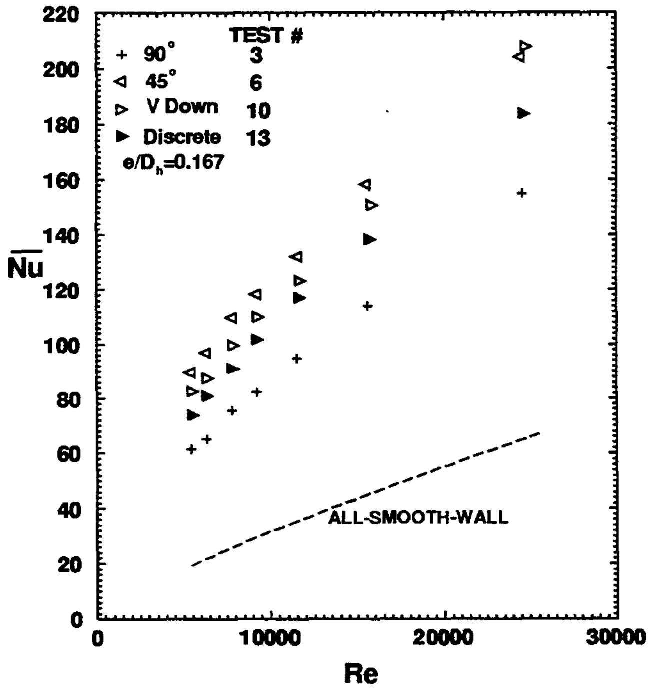

Figure 15 Comparison of Surface Average Nusselt Number for Four Rib geometries of 0.167 Blockage Ratio

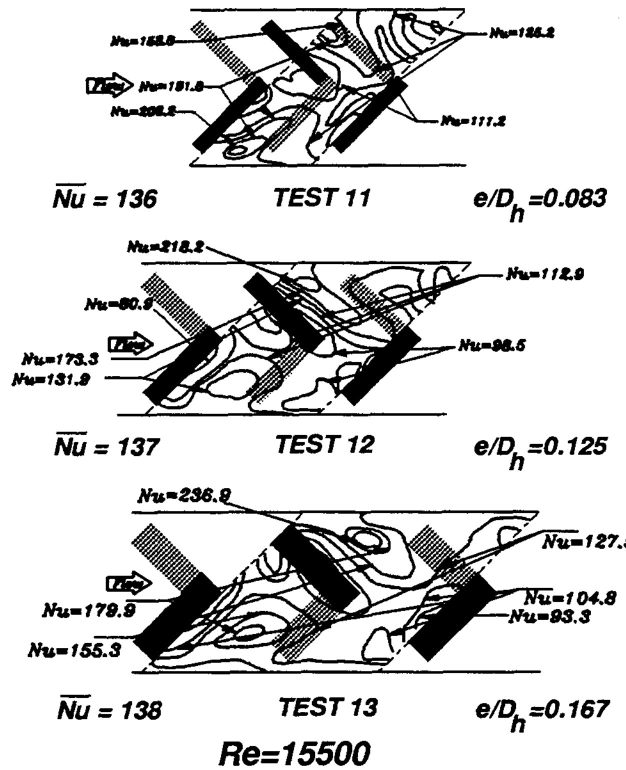

Figure 17 Representative Iso-Nu Contours for the 45° Discrete Ribs

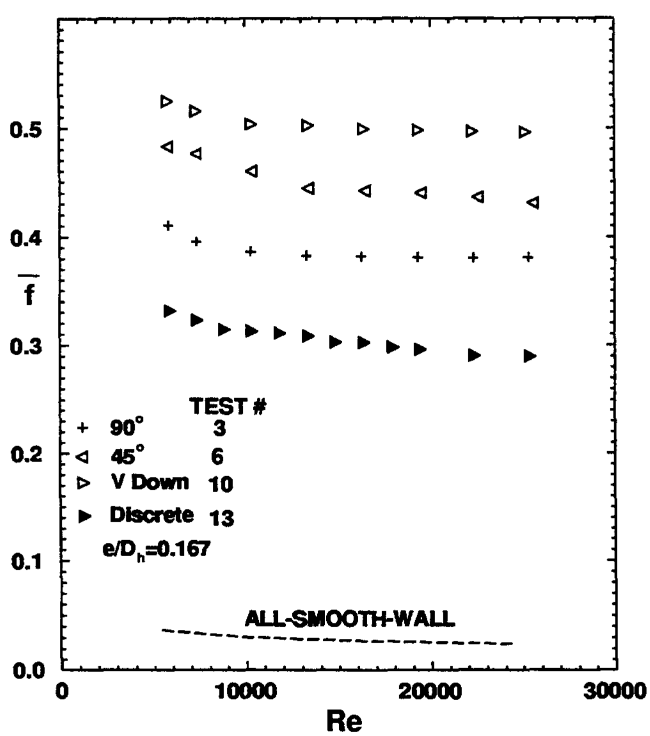

Figure 16 Comparison of Channel Average Friction Factor for Four Rib geometries of 0.167 Blockage Ratio

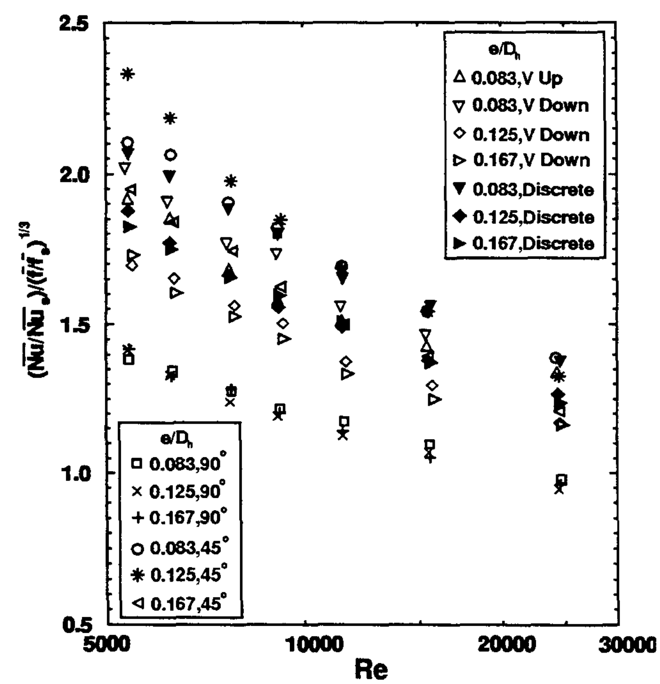

Figure 18 Thermal Performance of the Thirteen Rib Geometries

the ribs and smooth sidewalls (Figure 2). These gaps allowed channeling of some local air with little interaction with the ribs which results in lower center and endwall heat transfer coefficients as noted in Figure 17, compared to the V-shape iso-Nu distribution in Figure 7b. The surface-averaged heat transfer coefficients and friction factors for the 90°, 45°, V-shape and discrete ribs of smallest blockage ratio (0.083) are compared in Figures 10 and 11. Furthermore, as shown in Figure 12, the heat transfer enhancement for these geometries compare favorably with those of Han et al. (1991) of otherwise identical geometries except for their blockage ratio of 0.0625.

The surface-averaged heat transfer coefficients and friction factors for the 90°, 45°, V-shape and discrete ribs of two higher blockage ratios (0.125 and 0.167) are compared in Figures 13 - 16. First, it is observed that for these higher blockage ratios, compared with V-shape ribs, 45° ribs result in higher average heat transfer coefficients with lower pressure losses. Secondly, discrete ribs of all tested blockage ratios have less pressure loss and higher heat transfer enhancements than 90° ribs. Representative iso-Nu contours for the discrete ribs are shown in Figure 17. Again, considerable spanwise variations in heat transfer is observed due to the presence of secondary flows and the gap between the ribs.

As mentioned before, the thermal performance of all geometries tested are compared in Figure 18. It is seen that 90° ribs represent the lowest thermal performance and their thermal performance does not change significantly with blockage ratio. The 45° ribs have the highest thermal performance and the other two geometries (V-shape and discrete ribs) fall in between with the discrete ribs producing a higher thermal performance than the V-shape ribs.

CONCLUSIONS

A total of thirteen rib geometries representing three blockage ratios in a practical range and four different configurations were tested for heat transfer and friction variations. From this study, it is concluded that:

1) The 45° ribs and the lowest blockage discrete ribs had thermal performance which was the highest among the geometries tested in this investigation.

2) The 90° ribs represent the lowest thermal performance and their thermal performance does not change significantly with blockage ratio.

3) Low blockage ratio (e/D_h =0.083) V-shape ribs pointing downstream produced the highest heat transfer enhancement and friction factors. Amongst all other geometries with blockage ratios of 0.125 and 0.167, 45° ribs showed the highest heat transfer enhancements with friction factors less than those of V-shape ribs.

4) The discrete angled ribs, although inferior in average heat transfer coefficients to 45° and V-shape ribs, produce much higher heat transfer coefficients and lower friction factors compared to 90° ribs.

ACKNOWLEDGEMENT

The authors wish to express gratitude to Mr. James E. Hinds for his professional advice in preparing the final manuscript.

REFERENCES

1. Abuaf, N., Gibbs, R. and Baum, R., 1986, "Pressure Drop and Heat Transfer Coefficient Distributions in Serpentine Passages With and Without Turbulence Promoters," *The Eighth International Heat Transfer Conference*, Edited by C.L. Tien, V.P. Carey and J.K. Ferrel, pp. 2837-2845.

2. Burggraf, F., 1970, "Experimental Heat Transfer and Pressure Drop with Two Dimensional Turbulence Promoters Applied to Two Opposite Walls of a Square Tube," ASME, *Augmentation of Convective Heat and Mass Transfer*, Edited by A.E. Bergles and R.L. Webb, pp. 70-79.

3. Chandra, P.R., 1987, "Effect of Rib Angle on Local Heat/Mass Transfer Distribution in a Two Pass Rib-Roughened Channel," ASME Paper # 87-GT-94.

4. Chandra, P.R. and Han, J.C., 1989, "Pressure Drop and Mass Transfer in Two-Pass Ribbed Channels", *AIAA J. Thermophysics*, Vol. 3, No. 3, pp. 315-319.

5. Colburn, 1933, "A Method of Correlating Forced Convection Heat Transfer Data and a Comparison With Fluid Friction", *TRANS. A.I.Ch.E.*, Vol. 29, pp. 174-210.

6. Dittus, F.W. and Boelter, L.M.K., 1930, University of California, Berkeley, CA, *Publications in Engineering*, Vol. 2, p. 443.

7. El-Husayni, H., 1991, "An Experimental Investigation of Heat Transfer Coefficients in Stationary and Orthogonally Rotating Smooth and Turbulated Heated on One, Two and Four Walls," MS Thesis , Mechanical Engineering Department, Northeastern University, Boston, MA.

8. El-Husayni, H., Taslim, M.E., and Kercher, D.M., 1992, "Experimental Heat Transfer Investigation of Stationary and Orthogonally Rotating Asymmetric and Symmetric Heated Smooth and Turbulated Channels," ASME paper # 92-GT-189.

9. Fann S., Yang W.J., Zhang N., 1994, "Local Heat Transfer in a Rotating Serpentine Passage with Rib-Roughened Surfaces", *Int J. Heat and Mass Transfer*, Vol. 37, No. 2, pp. 217-228.

10. Han J.C.., Glicksman, L.R., and Rohsenow, W.M., 1978, "An Investigation of Heat Transfer and Friction for Rib Roughened Surfaces," *Int J. Heat and Mass Transfer*, Vol. 21, pp. 1143-1156.

11. Han, J.C., 1984, "Heat Transfer and Friction in Channels with Two Opposite Rib-Roughened Walls," *J. Heat Transfer*, Vol. 106, No. 4, pp. 774-781.

12. Han, J.C., Park, J.S., and Lei, C.K., 1985 "Heat Transfer Enhancement in Channels With Turbulence Promoters," *J. Engr. for Gas Turbines and Power*, Vol. 107, pp. 628-635.

13. Han, J.C., Zhang, Y.M., and Lee, C.P., 1991, " Augmentated Heat Transfer in Square Channels With Parallel, Crossed, and V-shaped Angled Ribs," *J. Heat Transfer*, Vol. 113, pp. 590-596.

14. Han, J.C., Zhang, Y.M., and Lee, C.P., 1992, " Influence of Surface Heat Flux Ratio on Heat Transfer Augmentation in Square Channels with Parallel, Crossed, and V-shaped Angled Ribs," *J.*

Turbomachinery, Vol. 114, pp. 872-880.

15. Kline, S.J. and McClintock, F.A., 1953, "Describing Uncertainty in Single-Sample Experiments," *Mechanical Engineering*, Vol. 75, pp. 3-8.

16. Lau, S.C., McMillin, R.D. and Han, J.C., 1990, "Heat Transfer Characteristics of Turbulent Flow in a Square Channel with Angled Discrete Ribs," *J. Turbomachinery*, Vol. 111, No. 2, pp. 117-123.

17. Lau, S.C., Kukreja, R.T. and McMillin, R.D., 1992, "Heat Transfer in a Square Channel with Staggered Discrete Ribs," *J. Thermophysics and Heat Transfer*, Vol. 6, No. 1, pp. 171-173.

18. Metzger, D.E., Fan, C.S., and Pennington, J.W., 1983, "Heat Transfer and Flow Friction Characteristics of Very Rough Transverse Ribbed Surfaces With and Without Pin Fins," *Proc. ASME-JSME Thermal Engineering Joint Conference*, Vol. 1, pp.429-436.

19. Metzger, D.E, Chyu, M.K. and Bunker, R.S., 1988, "The Contribution of On-Rib Heat Transfer Coefficients to Total Heat Transfer from Rib-Roughened Surfaces," *Transport Phenomena in Rotating Machinery*, Edited by J.H. Kim, Hemisphere Publishing Co.

20. Metzger, D.E., Fan, C.S., and Yu, Y., 1990, "Effects of Rib Angle and Orientation on Local Heat Transfer in Square Channels with Angled Roughness Ribs," *Compact Heat Exchangers: A Festschrift for A.L. London*, Hemisphere Publishing Co., pp. 151-167.

21 Moody, L.F., 1944, "Friction Factors for Pipe Flow," *Trans.* ASME, Vol. 66, p. 671.

22 Moffat, R.J., 1990, "Experimental Heat Transfer," *Proc. 9th Int. Heat Transfer Conf.*, Vol. 1, pp. 187-204.

23. Taslim, M.E. and Spring, S.D., 1988a, "An Experimental Investigation of Heat Transfer Coefficients and Friction Factors in Passages of Different Aspect Ratios Roughened With 45° Turbulators," ASME *HTD*, Vol-96.

24. Taslim, M.E. and Spring, S.D., 1988b, "Experimental Heat Transfer and Friction Factors in Turbulated Cooling Passages of Different Aspect Ratios, Where Turbulators are Staggered," AIAA-88-3014.

25. Taslim, M.E., 1990, "Application of Liquid Crystals in Heat Transfer Coefficient Measurement," *Proc. of IEEE ELECTRO/90*, Boston, MA.

26. Taslim, M.E. and Spring, S.D., 1991a, "An Experimental Investigation into the Effects Turbulator Profile and Spacing Have on Heat Transfer Coefficients and Friction Factors in Small Cooled Turbine Airfoils," Paper # AIAA-91-2033.

27. Taslim, M.E., Rahman, A. and Spring, S.D., 1991b, "An Experimental Investigation of Heat Transfer Coefficients in a Spanwise Rotating Channel With Two Opposite Rib-Roughened Walls," *J. of Turbomachinery*, Vol. 113, pp. 75-82.

28. Taslim, M.E., Bondi, L.A., and Kercher, D.M., 1991c, "An Experimental Investigation of Heat Transfer in an Orthogonally Rotating Channel Roughened with 45° Criss-Cross Ribs on Two Opposite Walls," *J. of Turbomachinery*, Vol. 113, pp. 346-353.

29. Webb, R.L., Eckert, E.R.G. and Goldstein, R.J., 1971, "Heat Transfer and Friction in Tubes with Repeated-Rib-Roughness," *Int J. Heat and Mass Transfer*, Vol. 14 pp. 601-617.